Structure and emplacement of mud volcano systems in the South Caspian Basin

Simon A. Stewart and Richard J. Davies

ABSTRACT

The term ''mud volcano system'' is coined to describe the set of structures associated with a constructional edifice (mud volcano) and feeder complex that connects the volcano to its source stratigraphic unit. Three-dimensional (3-D) seismic data from the South Caspian Basin are used to investigate the structural elements and evolution of these systems. Mud volcano systems initiate via early, kilometer-scale, biconic edifices termed ''pioneer'' cones. These are fed by fluidization pipes tens of meters in width. Subsequent kilometer-scale mud volcanoes grew via persistent extrusion, fed by numerous additional fluidization pipes injected in the country rock. This subvolcanic intrusion complex creates a densely intruded, cylindrical zone, similar in cross section to gryphon swarms observed at an outcrop onshore. Wall rock erosion and compaction of the intruded zone leads to the collapse of a downward-tapering cone enveloping the cylindrical zone, capped by ring faults that define a kilometer-scale caldera that downthrows the overlying mud volcano. Mud volcanoes get buried during basin subsidence and can look like intrusive laccoliths at first glance on seismic data. Reactivation of mud flow through a conduit system generates a stack of superimposed mud volcanoes through time. Large volcanoes continue to dewater during burial and may locally remobilize. This model of mud volcano evolution has similarities with igneous and salt tectonic systems. To reduce drilling and geologic uncertainty, mud volcano system extent and impacts on a reservoir can be assessed on 3-D seismic data.

INTRODUCTION

Thousands of mud volcanoes occur globally (Milkov, 2000), and they are of significance to a range of disciplines, including the oil industry. They represent an important global mechanism for degassing deeply buried sediments and contribute significant

Manuscript received March 7, 2005; provisional acceptance May 23, 2005; revised manuscript received October 24, 2005; final acceptance November 22, 2005.
DOI:10.1306/11220505045

AUTHORS

SIMON A. STEWART ~ *BP Azerbaijan, Chertsey Road, Sunbury on Thames, Middlesex TW16 7LN, United Kingdom; stewarsa1@bp.com*

Simon Stewart received his Ph.D. from the Imperial College London in 1992. In 1992–2000, he was seismic interpreter at Amerada Hess, in support of exploration and appraisal drilling in the North Sea. In 2000, he moved to BP and has since worked on structural geology and well planning in the Americas, Middle East, and the former Soviet Union. His special interest is in the integration of structural geology and seismic interpretation.

RICHARD J. DAVIES ~ *CeREES (Center for Research into Earth Energy Systems), Department of Earth Sciences, University of Durham, Science Labs, Durham DH1 3LE, United Kingdom*

Richard Davies received his Ph.D. from the University of Edinburgh in 1995. In 1995–2003, he was with Mobil and ExxonMobil, working on field development and exploration, the North Sea, the west of Shetlands, and the west Niger Delta deep-water slope. In 2003–2005, he was a senior lecturer in earth sciences at Cardiff University, United Kingdom. Currently, he is professor and director of CeREES (Center for Research into Earth Energy Systems), Durham University, United Kingdom. His special interest is in seismic-scale expression of fluid migration and diagenesis.

ACKNOWLEDGEMENTS

This article is published with permission of the Azerbaijan International Operating Company (AIOC) partnership. Views expressed here are solely those of the authors and not necessarily those of BP or any of the AIOC partners. R. J. Davies thanks Schlumberger for use of seismic interpretation software, as well as Rob Evans and Andy Robinson for discussions. This article was improved in light of the reviews made by B. Brister, R. Nelson, and B. Trudgill.

volumes of fossil methane to the atmospheric budget (Judd, 2005; Kvenvolden and Rogers, 2005). They are also potential but poorly understood geologic hazards to local communities and shipping and are commonly associated with petroleum systems. Uncertainties in the mud volcano system structure contribute to risk for wells drilled for oil and gas production because the mud is associated with poorly constrained pore pressure and fracture strength, factors that affect the stability and drillability of hydrocarbon industry boreholes (Ebrom et al., 2004). Reservoir compartmentalization caused by mud withdrawal at depth is also possible (e.g., Troll et al., 2002).

Most of the published work on mud volcanoes focuses on the geometry of mud volcano edifices (based on outcrop and well data) and the geochemistry of expulsed fluids (e.g., Lance et al., 1998; Milkov, 2000; Kopf et al., 2003; Murton and Biggs, 2003; Etiope et al., 2004). A relatively small proportion of published work has used seismic reflection data (Van Rensbergen et al., 1999; Graue, 2000; Cooper, 2001a, b; Yusifov and Rabinowitz, 2004). Here, we present the results of mapping three-dimensional (3-D) seismic data that link mud volcano edifices via their underlying feeder systems down to the in-situ source layer at depth.

Existing models of subsurface systems that feed mud volcanoes vary from bulbous diapirs (Brown, 1990) to steep diatremes (Pickering et al., 1988; Robertson and Kopf, 1998; Clari et al., 2004) and narrow vertical pipes (Graue, 2000; Planke et al., 2003), as reviewed by Kopf (2002). Noting that in the literature, the term ''mud volcano'' commonly refers to a constructional edifice, whether outcropping or buried (reviews by Dionne, 1973; Milkov, 2000), we use the term ''mud volcano system'' to describe the full 3-D structure from source to extrusives. Continuing a line of investigation begun by Brown (1990), who drew parallels between mud and igneous volcanism, Davies and Stewart (2005) showed that mud volcano systems in the South Caspian Basin have similarities with the subsurface structure of igneous volcanic centers (e.g., Francis, 1970; Lipman, 2000; Johnson et al., 2002). Similarities include the bicone-shaped volcanic edifice underlain by a ring complex consisting of a caldera and a downward-tapering cone of collapsed country rock (Davies and Stewart, 2005). However, Morley and Guerin (1996) show that as a result of mud being weak and mobile, there can also be similarities with salt tectonic processes and structures.

This study utilizes two-dimensional (2-D) and 3-D seismic data acquired by the hydrocarbon industry in the South Caspian Basin (Figure 1). These data image fully preserved, kilometer-scale mud volcano system examples, allowing us to build on previous studies (Cooper, 2001a, b; Davies and Stewart, 2005) and place mapped structural elements of the mud volcano systems from the South Caspian Basin into a context of how long-lived mud volcano systems evolve. After a summary of the database and regional setting, we describe an inventory of mapped and interpreted structural elements, concluding with an integrated process model of mud volcano system evolution based on these observations, drawing parallels with igneous and salt tectonic processes and structures. Because the focus of this article is on mud volcano system geometry, we employ a broad definition of mud encompassing all intrusive and extrusive material sourced from the in-situ layer at depth (Maykop Formation).

DATABASE

The seismic data were acquired using conventional towed streamer and ocean bottom cable technology (Davies et al., 2004). Vertical resolution of the 3-D data is tens of meters, with spatial sampling of 12.5 m (41 ft). Examples from regional 2-D seismic data have been published separately (Yusifov and Rabinowitz, 2004). The 3-D seismic data have been prestack depth migrated and tied to drilled wells prior to final seismic interpretation. Two-dimensional seismic data are poststack time migrated. The vertical scale on all 3-D seismic data is depth; 2-D data are in two-way traveltime. Some locations of seismic sections and structures in this article are not shown for proprietary reasons.

REGIONAL SETTING

The South Caspian Basin is bounded in the north by a northwest-southeast–striking, Mesozoic- to Paleogene-age accretionary prism overlain by Tertiary-age folds (Figure 1) (Jackson et al., 2002; Allen et al., 2003; Knapp et al., 2004). These folds balance ongoing shortening across the underlying accretionary prism and deform up to 15 km (9 mi) of Oligocene to Holocene siliciclastics; they detach on overpressured mud of the Maykop Formation (Figure 1) (Brunet et al., 2003). Mud volcano systems are broadly synchronous with these large-scale folds in the study area (Figure 1), showing that the tectonic context of mud volcanoes described here is regional compression. Detailed mapping at oil-field scale in

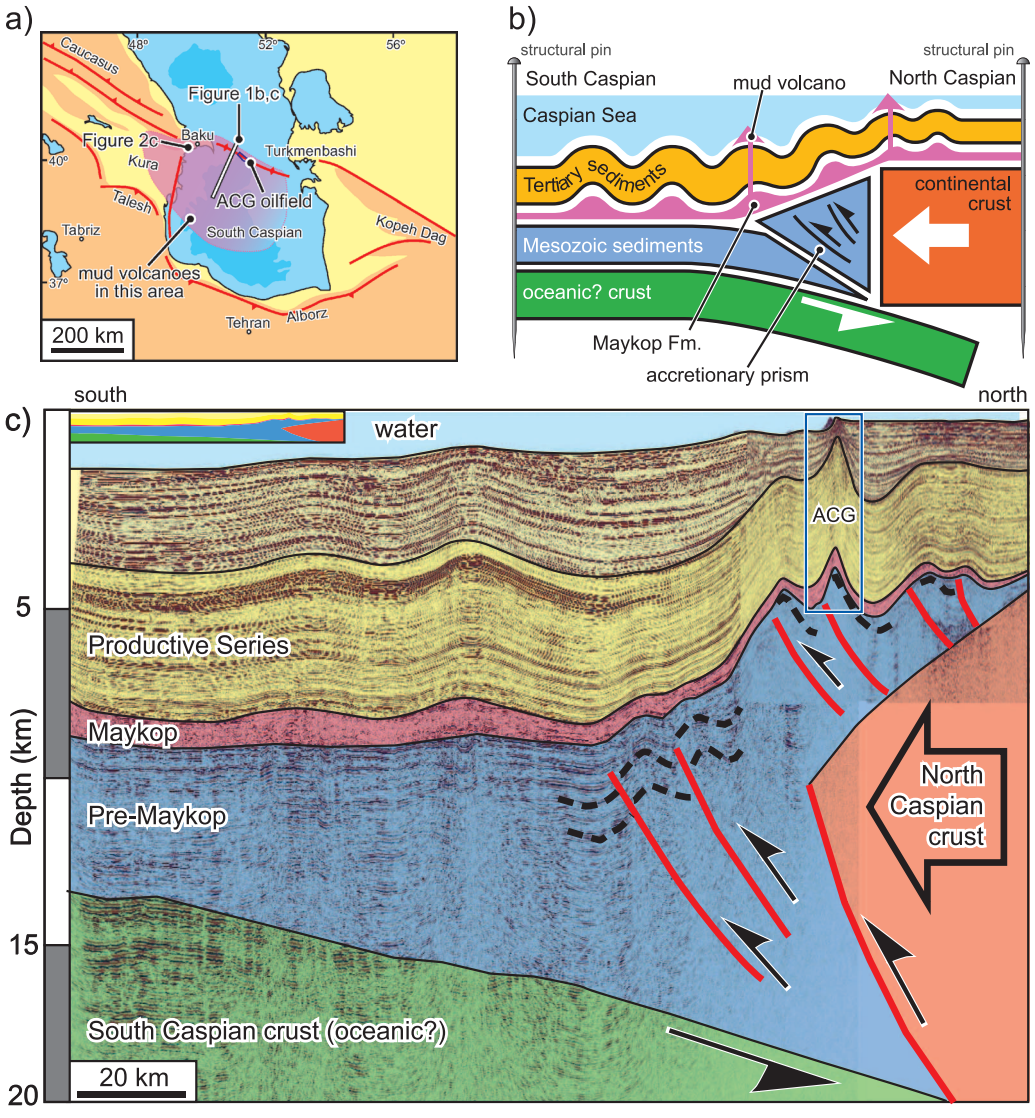

Figure 1. (a) The South Caspian Sea showing locations relevant to this article. The ACG (Azeri-Chirag-Gunashli) oil field is the principal study area. Mud volcano occurrence is poorly constrained in the east and south. Colors are bathymetry (blues) and topography (yellow-orange; orange is highlands). (b) Tectonostratigraphic elements in the South Caspian (cartoon interpretation of part c) location marked in (a). The Maykop Formation is the source of mud and petroleum in this basin. The section is oriented north on the right. (c) Regional 2-D reflection seismic line showing main tectonostratigraphic elements, location in (a), approximately 6× vertical exaggeration. Inset shows the interpretation at vertical = horizontal scale. Blue box marked ACG oil field is the principal study area of this article.

the fold structures reveals minor faults with extensional geometry. Subsets of these are en echelon in map view, indicating a minor element of Neogene strike slip that ties to historical P-wave data (Knapp et al., 2004), but integrating mud volcano systems with this level of detailed kinematic analysis is beyond the scope of this article.

Lithologic data from boreholes show that strata penetrated by the mud volcano systems are dominantly lacustrine, and that the mud was extruded into shallow water (<100 m; <330 ft). Extremely rapid rates of deposition (up to 2 km/m.y. [0.6 mi/m.y.]) generated overpressure via disequilibrium compaction (Narimanov, 1993). The lowest part of the studied succession is the Oligocene- to Miocene-age Maykop Formation, the source of the mud volcano systems (Inan et al., 1997), and has been buried to depths of 3–7 km (1.8–4.3 mi) in the study area (Figure 1). The Maykop Formation has variable present-day thickness but was originally approximately 1 km (0.6 mi) in the study area (Figures 2, 3). It is a key factor in basin tectonics, forming an upper structural detachment (roof thrust) to the thrust system of the accretionary prism (Figure 1). Above the upper detachment, shortening is balanced by detached buckle folding of the upper plate well out into the basin beyond the tip of the accretionary prism (Figure 1b). In addition to sourcing the mud volcano systems, the Maykop shales have been generating hydrocarbons since the Pliocene and are the source for billion barrel reserve oil fields that trap in the buckle folds above the autochthonous Maykop shale detachment (Figure 1) (Bagirov et al., 1997).

Extruded xenoliths and isotopes indicate that fluids and gases are also fed into the petroleum system from

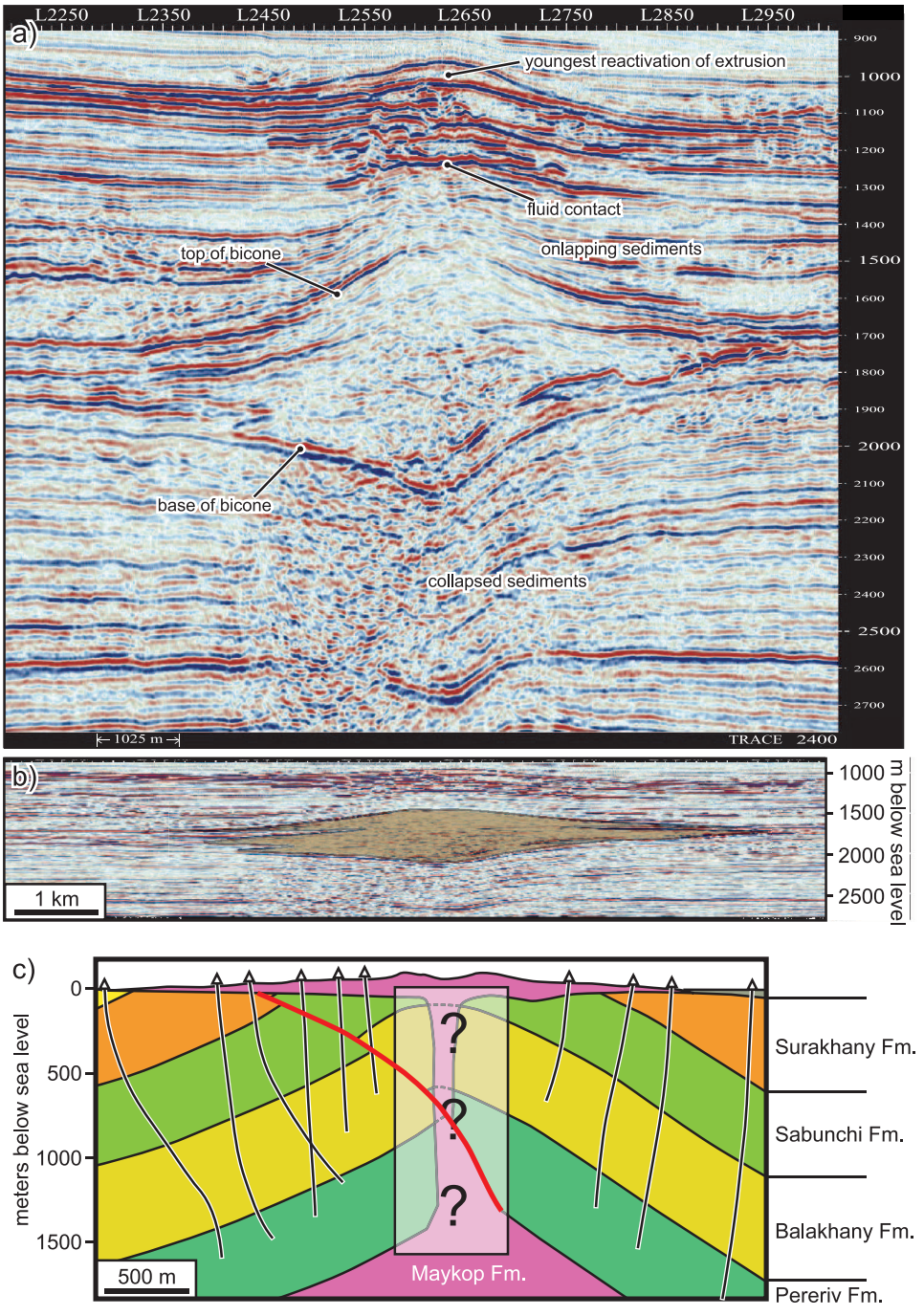

Figure 2. (a) Typical seismic image of a buried mud volcano edifice with bicone form (the top is the upward-pointing cone, and the base is the downward-pointing cone). (b) Same section as (a) displayed approximately vertical = horizontal; mud volcano is shaded. (c) Section through a mud volcano associated with an oil field onshore Azerbaijan (location in Figure 1a). Compare the scale and shape with the seismically imaged example in (b). The section is constructed from stratigraphy in drilled wells. The architecture of feeder system connecting to the in-situ Maykop Formation is poorly constrained.

the underlying, pre-Maykop strata, i.e., the accretionary prism (Figure 1) (Kopf et al., 2003). Association of fluid expulsion and mud volcanism with accretionary prism thrust systems is a common feature of plate boundaries (Bray and Karig, 1985; Talbot and von Brunn, 1989; Brown, 1990; Kopf et al., 2001), but the distribution of mud volcanoes extends hundreds of kilometers south of the leading edge of the accretionary prism (Figure 1), indicating that dewatering of that accretionary prism is not a primary source of fluids for mud volcanism in the basin. Present-day water depth ranges from 100 to 500 m (330 to 1640 ft) across the study area.

SEISMIC INTERPRETATION

Mud volcano systems are described here in terms of structural elements. We start with the shallowest structural levels (extruded, allochthonous mud), finishing

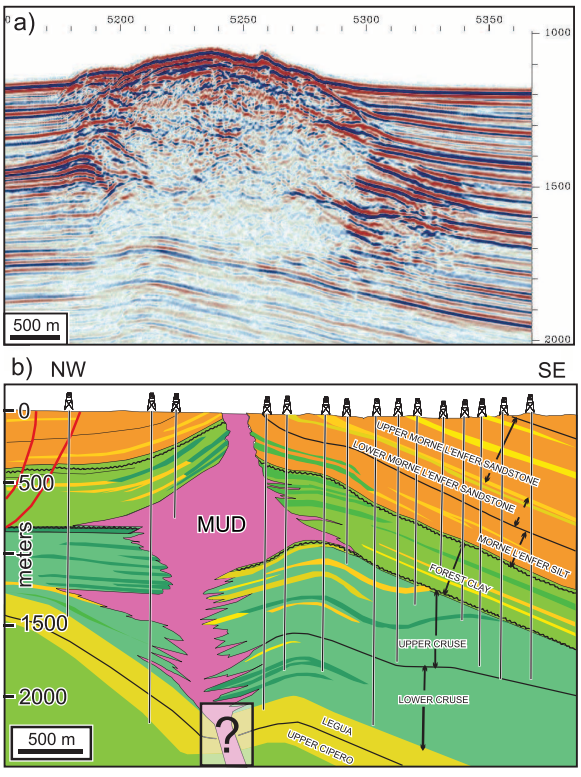

Figure 3. (a) A South Caspian volcanic edifice showing the margins interdigitating with adjacent sediments, reflecting the variation in the rate of extrusion relative to background sedimentation. (b) Buried mud volcano with interdigitating margins, Trinidad, reconstructed from well control (modified from Deville et al., 2003). As in Figure 2c, the subvolcano structural elements are poorly constrained.

with structures in the roof and base of the autochthonous mud-source layer. Everything underneath the extrusive edifice was grouped into a volcano root zone by Davies and Stewart (2005). Here, we describe the subvolcanic elements of the system in more detail and define ''root complex'' as the area in the immediate vicinity of, and including, the mud source. Table 1 records measurements of mud volcano systems mapped in detail within the ACG (Azeri-Chirag-Gunashli) oil field.

Volcano

Published mapping of mud volcanoes onshore Azerbaijan and elsewhere documents a characteristic conic shape with upper surface slope angles typically ranging from 2 to 20° (Figure 2) (Jakubov et al., 1971; Hovland et al., 1997). Seismic imaging of the base and lateral margins of volcanic edifices reveals a variety of morphologies and internal structures. Although exposed examples of mud volcanoes exhibit significant meter-scale complexity (Hovland et al., 1997; Murton and Biggs, 2003; Planke et al., 2003), seismic data show that at a kilometer scale, the simplest edifices can be described as radially symmetrical bicones (two cones placed base to base), similar in cross section to shield-type igneous edifices (Figure 2a) (cf. Walker, 1988). The lower, downward-pointing cone cannot be a depth-imaging artifact arising from low velocity in the mud relative to adjacent sediments (velocity pushdown of a flat base) because, for this to be true, the entire vertical thickness of mud in the bicone would require an average sonic velocity significantly less than that of water (calculation is based on the bicone imaged in Figure 2a and sediment velocity outside the mud volcano of 2200 m s^{-1} [7217 ft s^{-1}], from well control). Radially symmetrical bicones (Figure 2) can occur in groups that are stacked vertically with a common root system, the stacked bicones separated by concordant seismic reflections (representing background sedimentation) that onlap the individual bicone margins (Figure 3a). A stack of overlapping bicones creates an edifice with a Christmas tree appearance in cross section (Figure 3b), a term first used in the Gulf of Mexico in the context of emergent salt structures (Yeilding and Travis, 1997).

Table 1. Dimensions of Mud Volcano System Elements Mapped in Detail in This Study*

Volcano	Mud Volume (km^3)	Caldera Depth (m)	DTC** Width (km)	DTC** Height (km)	Asymmetric Caldera?	Faulted Caldera?	Stacked Cones
1	22.5 (Chirag)	600	1.6	1.9	Yes	Yes	5
2	2.75 (Azeri)	180	1.1	2.6	Yes	Yes	2
3	4.1 (Azeri)	340	4.0	2.2	Yes	Sag	2
4	2.1 (Gunashli)	140	0.9	2.6	Yes	Yes	1
5	2.2 (Gunashli)	210	0.9	1.3	Yes	Yes	1

*No corrections for compaction.
**DTC = downward-tapering cone.

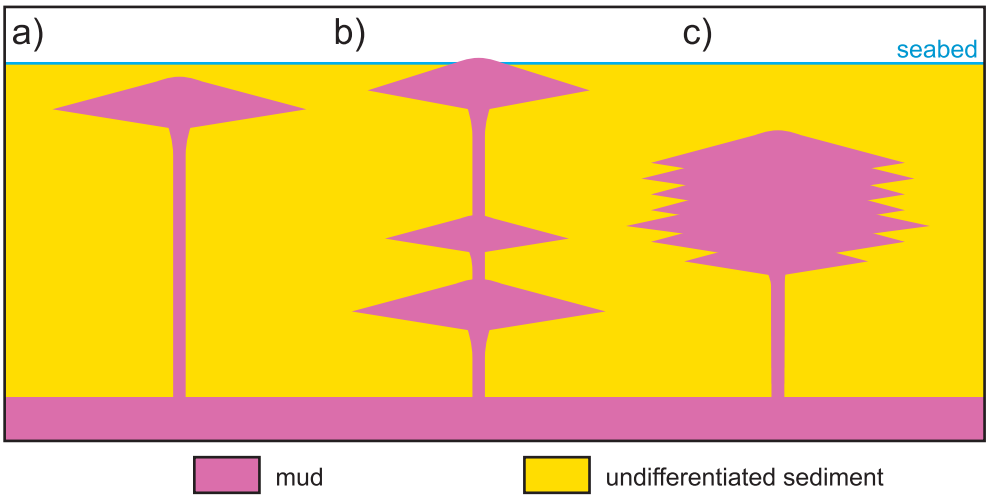

Figure 4. Cartoon showing end-member geometries of stacked mud volcanoes in a subsiding basin. Volcanoes are kilometer scale. No subvolcanic structure is implied. (a) A single mud volcano bicone at a shallow structural level, connected by a long feeder to the mud source. (b) Episodic reactivation, edifice building, and burial create a stack of bicones of various sizes, the youngest shown here yet to be fully buried. (c) A single episode of pulsed extrusion, punctuated by brief periods of relatively high rates of background sedimentation, creates an interdigitating margin and Christmas tree appearance. Geometries (a) or (c) could be misinterpreted as plutonic intrusions.

Searching downward through the 3-D seismic data below emergent or shallow-buried volcanoes, deeper buried bicones are commonly imaged above the in-situ mud source (Maykop Formation). Widely or irregularly spaced vertical stacking of these are some of many possible variations on the Christmas tree pattern (Figure 4). The stacking sequence is a visual record of the reactivation history.

Pipes

Seismic imaging of small, buried bicones shows that they lie at the upper termination of steep discontinuities that are localized in plan view and, therefore, pipelike in 3-D (Figure 5) (Fowler et al., 2000; Graue, 2000). The possibility of such pipes being geophysical imaging artifacts must be ruled out. Tall, narrow zones of low signal-to-noise ratios that might be misinterpreted as geological features could be produced below an energy-absorbing feature (Aminzade et al., 2001). The following observations argue against this. Seismic reflection character (e.g., continuity with reflections distant from the volcano) below large volcanoes mapped in this study is generally good, indicating that the energy absorption by the volcano is relatively low (Figure 2a). Volcanoes with a diameter significantly less than the streamer length of the seismic acquisition apparatus (4 km; 2.5 mi) will be undershot and will not be seen by a large proportion of the seismic energy that is stacked into the final image. All of the steep features interpreted as pipes in this study are breaks in seismic continuity instead of features with measurable width. Field examples of breccia pipes can be up to 100 m (330 ft) in diameter (e.g., Freeman, 1968; Kurszlaukis and Barnett, 2003), albeit in more competent country rock than present in the South Caspian examples. Three-dimensional seismic technology employed here is, however, not capable of imaging subvertical structures of this diameter.

Davies and Stewart (2005) noted the presence of a small, extrusive bicone fed by a pipe, at a low structural level in the mud volcano system mapped here as example 1 (Figure 5). This was termed a ''pioneer cone'' and interpreted as a precursor to the location and emplacement process of the later, larger mud volcano system (Davies and Stewart, 2005).

Caldera

The volcanic bicones mapped in this study are underlain by calderas that are 140–600 m (459–1968 ft) in depth and 1–2.5 km (0.6–1.5 mi) in diameter, measured at the base of the extrusive bicone (Table 1). Calderas at this scale have also been reported in association with mud volcanism on the Mediterranean Ridge (Kopf and Behrmann, 2000) and Niger Delta (Graue, 2000). The South Caspian Basin subvolcano calderas display various degrees of symmetry but fit within the range of caldera geometries described in reviews of geological processes that produce circular collapse structures (Branney, 1995; Roche et al., 2000; Cole

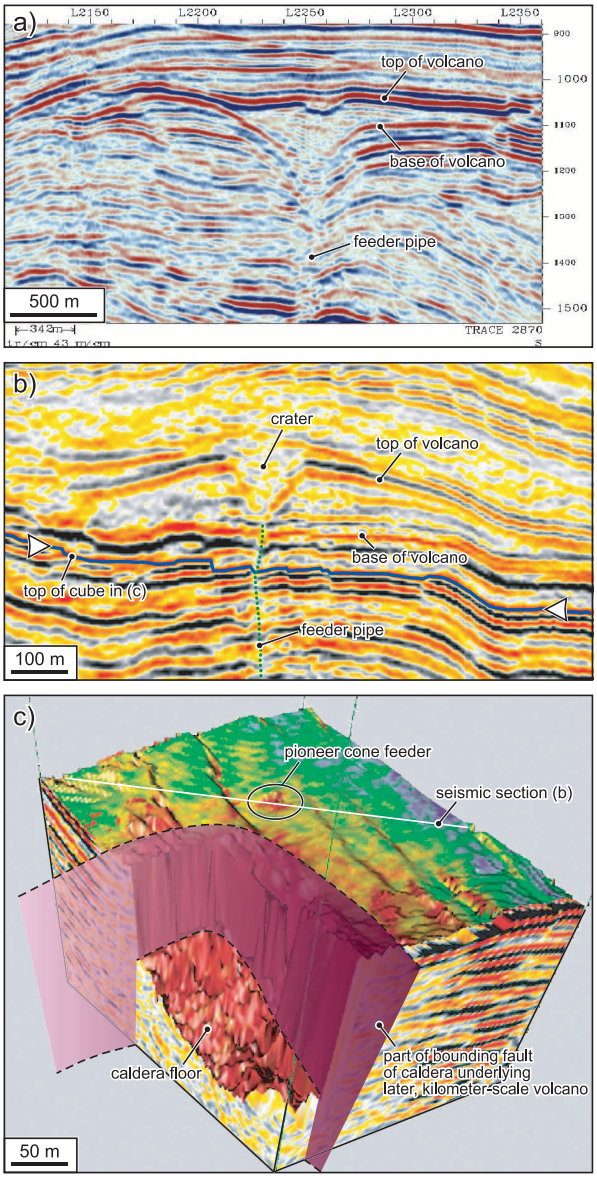

Figure 5. Pioneer cones and underlying feeder structure. All seismic data have a vertical exaggeration of approximately 2×. (a) Cone with well-developed feeder pipe structure. (b) Kilometer-scale edifice with summit crater. Reflectors below the mud volcano are offset by normal faults and cut by a feeder pipe. (c) Three-dimensional cube whose top surface is clipped to a reflector close to the base mud volcano (see b), draped by its seismic amplitude. Warm colors are high, and cool colors are low. View is toward the northwest. The cube also contains a part of the main caldera wall, 150 m (492 ft) away from the circular pipe that fed the pioneer volcano.

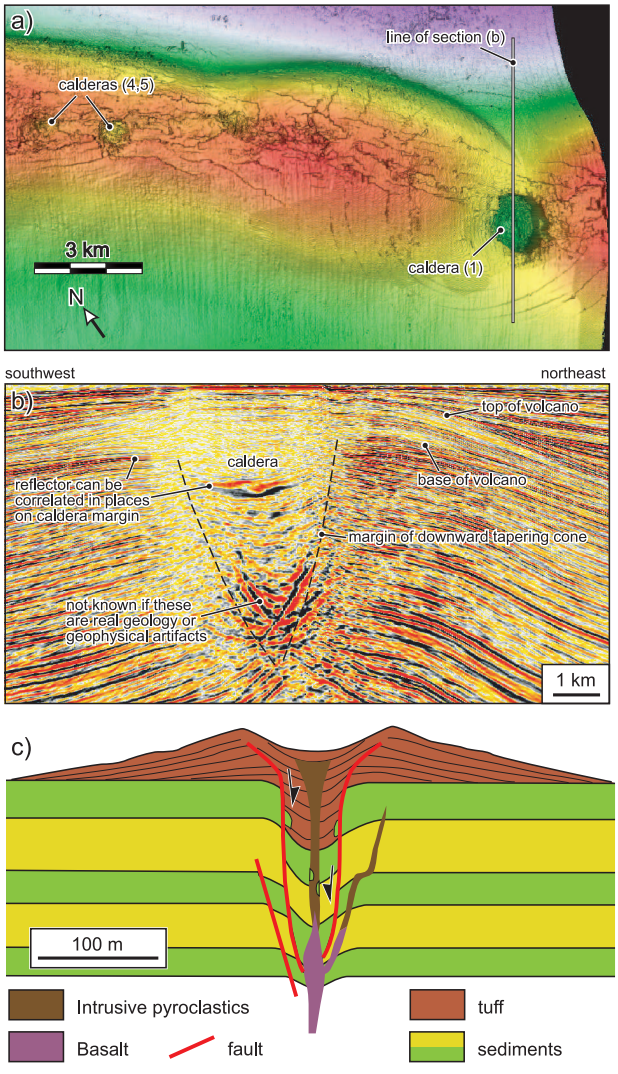

Figure 6. Caldera structures below volcanoes. (a) Shallow seismic reflection showing the periclinal form of the ACG (Azeri-Chirag-Gunashli) oil field and kilometer-scale calderas. Each caldera underlies a mud volcano bicone. Warm colors are high, and cool colors are low. Caldera numbers are keyed to Table 1. (b) Seismic section through a mud volcano bicone showing underlying caldera, located in (a). (c) Idealized section through igneous volcano with underlying caldera, assembled from field exposures of Carboniferous strata in east Scotland by Francis (1970). Compare with the structure of mud volcano systems throughout this article.

et al., 2005). Furthermore, the geometries, proportions, and relationships between the caldera and overlying volcanic edifice are very similar to those pieced together from field exposures of igneous systems (Figure 6) (Francis, 1970; Lipman, 2000; Johnson et al., 2002).

Fault displacement varies around the circumference of the caldera in example 1, from no resolvable offset in the southwest to approximately 400 m (1312 ft) displacement in the northeast. The fault zone is steep (about 75°). Other examples are similar in size but are saglike depressions (termed "downsags" by Cole et al., 2005), with monoclinal folds instead of seismically resolved faults on their margins. All caldera boundaries

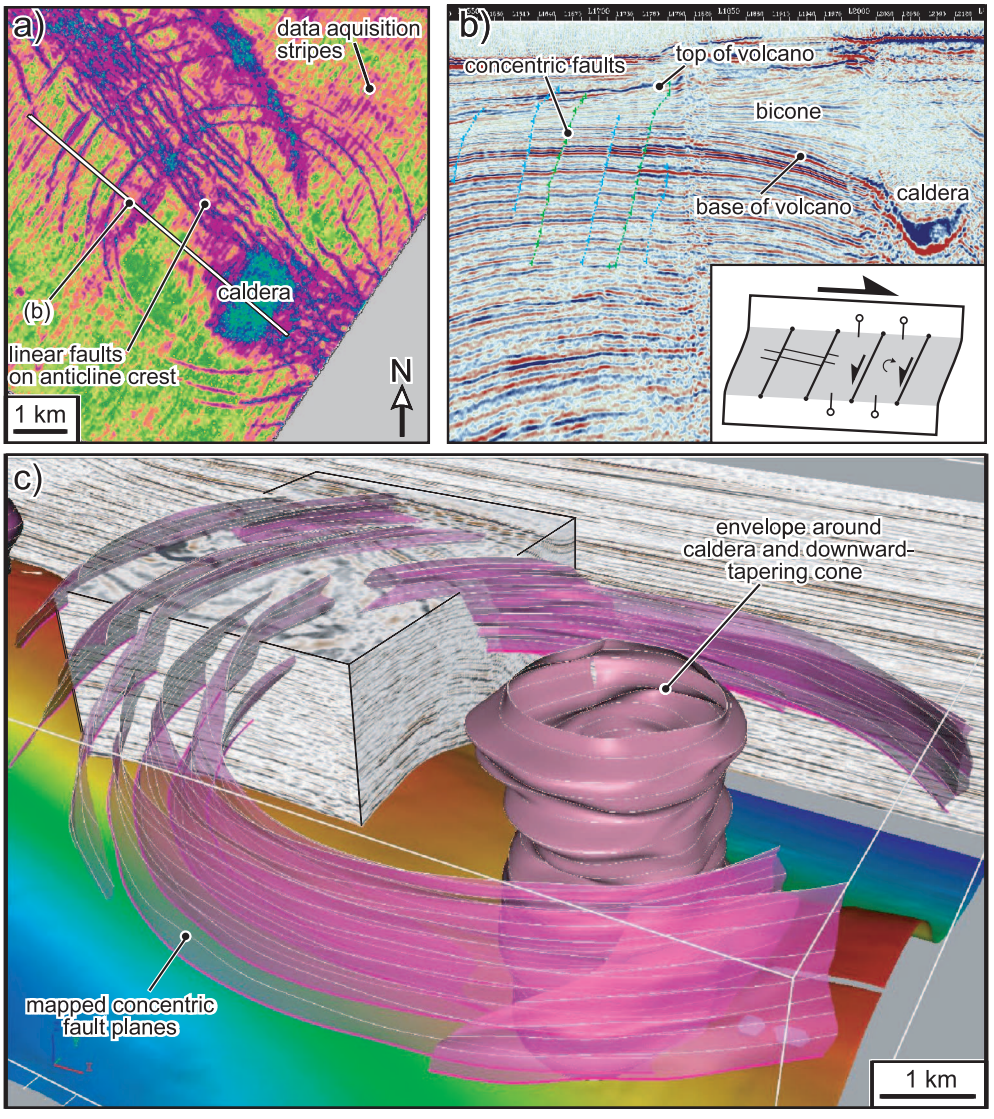

Figure 7. Unusual concentric ring faults surrounding a subvolcanic caldera. (a) Map of the concentric ring faults based on the disruption of a shallow seismic reflection amplitude (top Surakhany Formation). Warm colors are high, and cool colors are low, with purple highlighting (low) seismic amplitude. The linear fault set is associated with the outer arc extension of the anticline. (b) Seismic section through concentric faults (location in part a). Inset: kinematic interpretation of the section based on fault facing, tip geometry, and regional surface dip. (c) Three-dimensional view of the concentric fault system and margins of the caldera with downward-tapering cone. Elements of the seismic reflection cube are left to indicate the quality of seismic data on which the interpretation is based.

mapped in this study dip inward toward the caldera. Multidisciplinary literature indicates that bounding faults can face toward or away from the subsiding zone, but there appears to be no agreed model accounting for the polarity of caldera-bounding faults at the time of writing (Branney, 1995; Ge and Jackson, 1998; Malthe-Sørenssen et al., 1999; Roche et al., 2000). Caldera floors mapped in this study generally have a concave-up dish shape (Figure 6). The calderas mapped here are generally not concentric with overlying volcanoes. We offer an explanation below.

Antithetic Concentric Ring Faults

Uniquely in this study, the caldera below mud volcano 1 is surrounded by 14 minor extensional ring faults that cut the basal surface of the volcanic edifice, at a radial distance of 0.5–10 km (0.3–6 mi) from the caldera wall (Figure 7). In cross section, the faults are planar, have displacements of up to 30 m (98 ft), and dip at 45° relative to bedding. Twelve of the fourteen faults face away from the caldera and are, therefore, antithetic to the caldera margin faults. The lower fault tip lines are between 380 and 1100 m (1246 and 3608 ft) below the base mud volcano surface, and the upper fault tip lines are less than 200 m (660 ft) above it. The outermost ring fault is 9.1 km (5.6 mi) in diameter. They are concentric with the overlying bicone. They are a subtle but distinctive feature of this particular example and have not been recognized in any of the other mud volcano systems described here or, to the best of our knowledge, anywhere else. Applying a bookshelf fault kinematic model (e.g., Stewart and Argent, 2000), we interpret these faults as representing shear at the base of the

bicone toward its central axis, accommodating lateral compaction of the edifice muds (figure 3 of Davies and Stewart, 2005), a process that could be termed ''gravity contraction.'' We speculate that the occurrence of these features, in association with this particular example, may be related to it being the largest volcano mapped in this study, thus producing the highest magnitude of shear on the inclined basal bicone surface, and that shear was accommodated by seismically resolvable faults.

Downward-Tapering Cones

We use the term ''downward-tapering cones'' to describe steep-sided, cone-shaped complexes of collapsed country rock and intrusives that underlie the mapped calderas (Figure 8). Downward-tapering cones are described separately from calderas here but could have been bracketed as the underlying structure of the calderas described earlier. The description is separated here because, in some instances, the downward-tapering cones do not obviously terminate upward at calderas; for example, there may be steep pipes and disrupted strata but no caldera collapse. Where calderas are present, they form the top of the downward-tapering cone. Below example 1, the downward-tapering cone is 1.6 km (0.99 mi) wide at the top (i.e., the caldera) and about 100–300 m (330–984 ft) wide at its vertex. The vertex is mapped approximately 1.9 km (1.2 mi) below the floor of the caldera and some 200 m (660 ft) above the Maykop Formation. The connection to the Maykop Formation is not clearly imaged. The internal structure of the downward-tapering cone can be continuous or somewhat broken reflections with concave-upward geometry concordant with the overlying caldera floor or base mud volcano reflectors. Seismic reflections in the downward-tapering cone below caldera 4 describe a structure of 100-m (330-ft)-scale coherent blocks separated by a rather irregular fault pattern (Figure 8), similar to analog models of piecemeal caldera collapse (Troll et al., 2002). Strata outside the cone are relatively undeformed; the stratal reflections terminate against the edge of the conical fault system, which is sharply defined in this example.

Rim Syncline

A zone of sagged strata occurs directly above the area of depleted mud source (Figures 8, 9). The sagged zone surrounds the downward-tapering cone from the top of the mud source upward, until it defines the inward-dipping base surface of the extrusive bicone. This type of dish-shaped low, which forms a plan-view halo around an intrusion, has long been recognized in association with salt withdrawal (e.g., Trusheim, 1960; Vendeville, 2002), where it is termed a ''secondary rim syncline.'' As with salt structures, it should be possible to volumetrically balance depleted zones with rim synclines and extruded material (incorporating compaction and dewatering). Rim synclines might affect hydrocarbon reservoirs by imposing a local structural low, perhaps compartmentalizing the reservoir (e.g., Maione, 2001), albeit to a lesser extent than in the central caldera or downsag.

Root Complex

Downward-tapering cones terminate at or close to the top of the Maykop Formation (Figure 8a). We collectively term ''root complex'' as the structure that connects the downward-tapering cones to the mud source, the structure in the mud source itself, and the deeper structure that manifests at the base of the mud-source layer.

Depletion Zone

Mud volcano system 3 is centered above a thinned region of the underlying Maykop Formation. This isopach thin is elongate in plan view and covers an area of 150 km^2 (57 mi^2) (Figure 9). We interpret this thin region as resulting from mud evacuation to the overlying mud volcano, an interpretation making this zone analogous to salt isopach thins caused by drainage into diapirs (Trusheim, 1960). The depletion zone is located above a northwest-southeast–striking fault-related anticline in the pre-Maykop strata (Figure 9). At higher structural levels, the caldera margins are coincident with the thinnest section of the Maykop shale (Figure 9).

Basement Structure

The base of the source layer reveals several linear trends that we interpret as leading edges of thrust sheets emerging from the accretionary prism that separates the north and south Caspian plates (Figure 1) (Jackson et al., 2002; Allen et al., 2003; Knapp et al., 2004). Mud volcano system 3, in common with others on the Apsheron anticline trend, lies above the crest of the underlying accretionary prism thrust system. The depleted

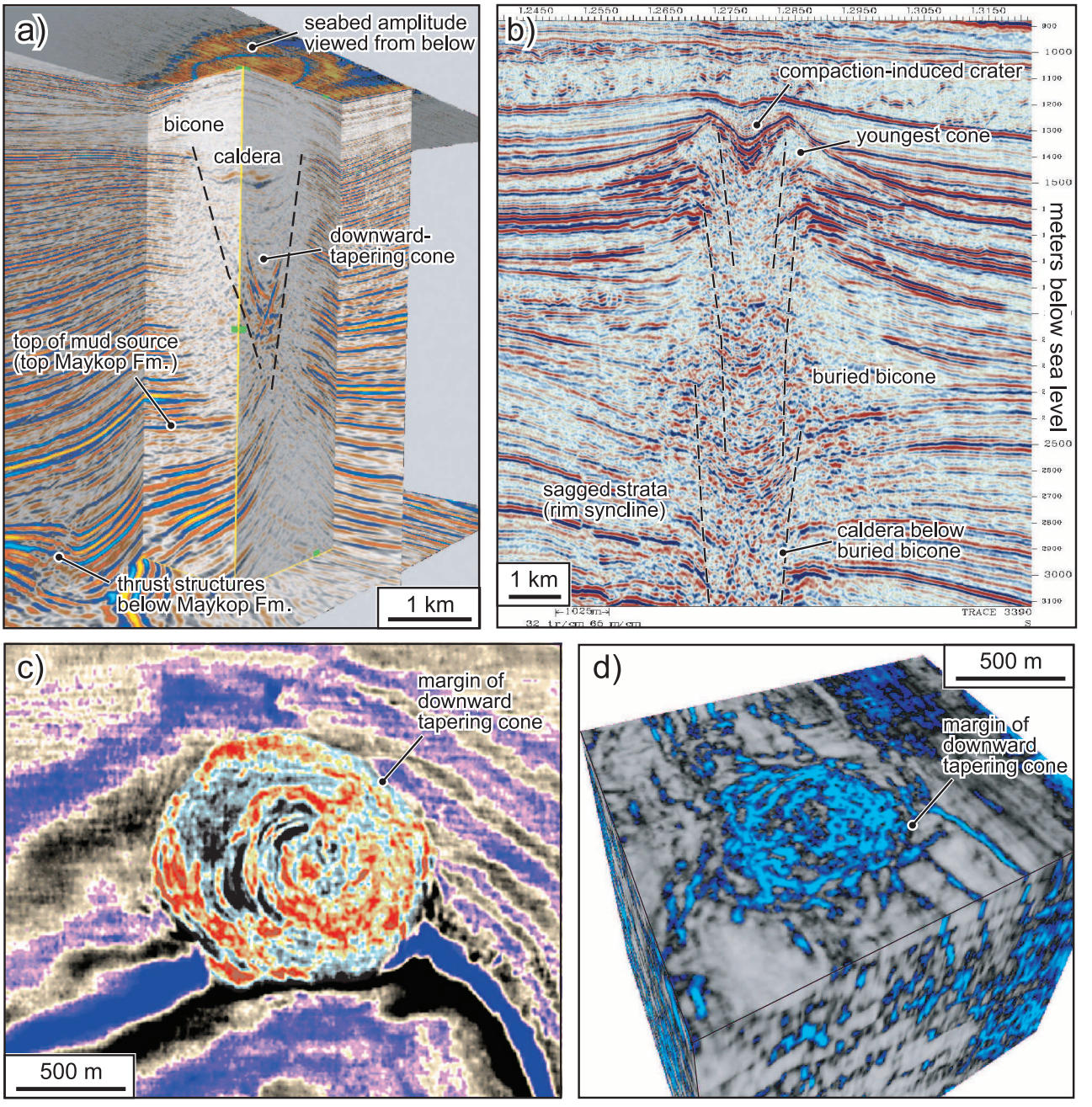

Figure 8. Calderas and downward-tapering cones of structure below mud volcanoes. (a) Cutaway seismic cube through a mud volcano system (example 1), also shown in Figure 6a and b, underlain by a caldera and downward-tapering structural cone. The view is to the northwest. (b) Stacked mud volcanoes and associated caldera collapse zones. The caldera stack defines a steep zone of subsidence that has propagated upward to form a pronounced crater on top of the youngest volcano. (c) Horizontal seismic section (depth slice) through a downward-tapering cone, showing an abrupt change from regional structure to faulting and folding of strata in the downward-tapering cone. (d) Seismic coherency data emphasizing stratal discontinuities in mud volcano system 4. The cube is located below the mud volcano and contains a downward-tapering cone. Discontinuities (bright blue) can be interpreted as faults and fracture zones. This visualization of structural complexity can be useful in well planning through or around mud volcano substructure.

zone is centered on the fold hinge line (Figure 9), and the conduit is located above the thrust. However, this is not a general association in the South Caspian Basin because mud volcanoes are also distributed well to the south of the accretionary prism and associated thrust sheets.

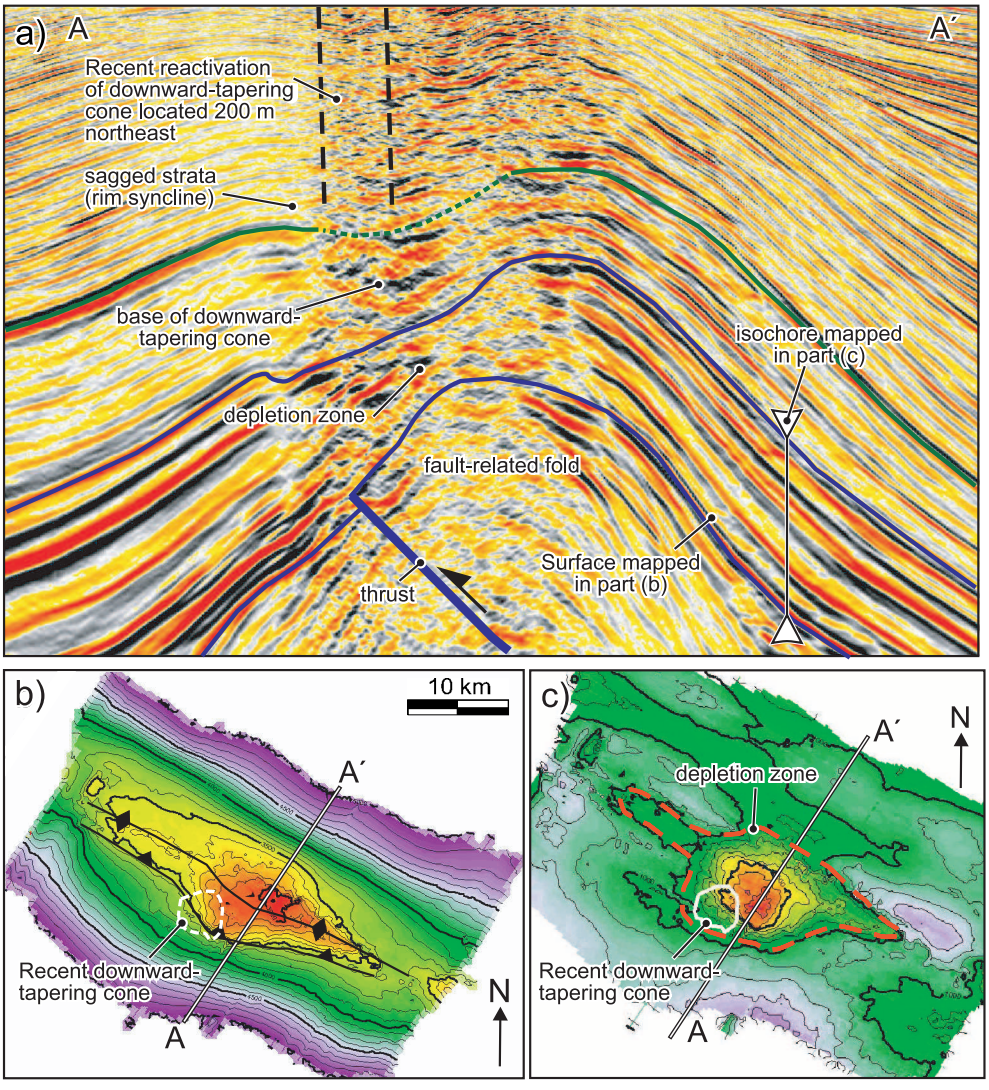

Figure 9. Root complex of mud volcano system example 3, where the downward-tapering cone connects to the mud-source layer, and related basement structure. (a) Representative seismic line showing a fault-related fold and significant thinning of the source unit in cross section. (b) Map of the top of the Maykop structure, showing the geometry of the basement fold and interpreted position of associated thrust fault. The downward-tapering cone is located above the thrust fault instead of the thrust-propagation fold hinge line. Warm colors are high. (c) Isochore (vertical thickness) map of the Maykop Formation. Dashed red line delineates the region where depletion has occurred. Warm colors indicate thinning.

PROCESS MODEL FOR MUD VOLCANO SYSTEMS

The mapping presented here supports the conclusions of Cooper (2001a, b) that a model of balloonlike mud diapirism mirroring salt diapir emplacement processes does not fully account for mud volcano system geometry in the South Caspian Basin. We have found that a key part of the process, absent from salt diapirism but common to igneous settings, involves sediment and fluid being transported upward through a conduit system with several distinctive structural elements such as downward-tapering cones of downfaulted country rock, steep narrow pipes, and calderas. This system feeds extrusive bicones that have process and geometric similarities to passive salt diapirs (Koyi, 1998; Rowan et al., 2003).

Extrusive mud volcanoes can become buried to form volumes of allochthonous mud at shallow structural levels that could be misinterpreted as intrusive mud diapirs or even appear as such on poor-quality seismic data that fails to image the base mud volcano (Cooper 2001a, b). Here, we synthesize the mapping described so far in this article into a process model for evolution of mud volcano systems in the South Caspian Basin (Figure 10).

The earliest manifestation of mud volcanism is an individual, pioneer bicone fed by a steep, discrete fluidization pipe (probably tens of meters in width) or diatreme that penetrates up to the free surface from the overpressured mud source (Kopf and Behrmann, 2000; Kopf, 2002; Davies and Stewart, 2005). Diatremes are steep fluidization conduits that intrude, erode, and replace country rock, widely described in relation to igneous intrusions (e.g., Lorenz, 1975; Kurszlaukis and Barnett, 2003). The term has also been used in relation to mud volcano evolution in sedimentary basins

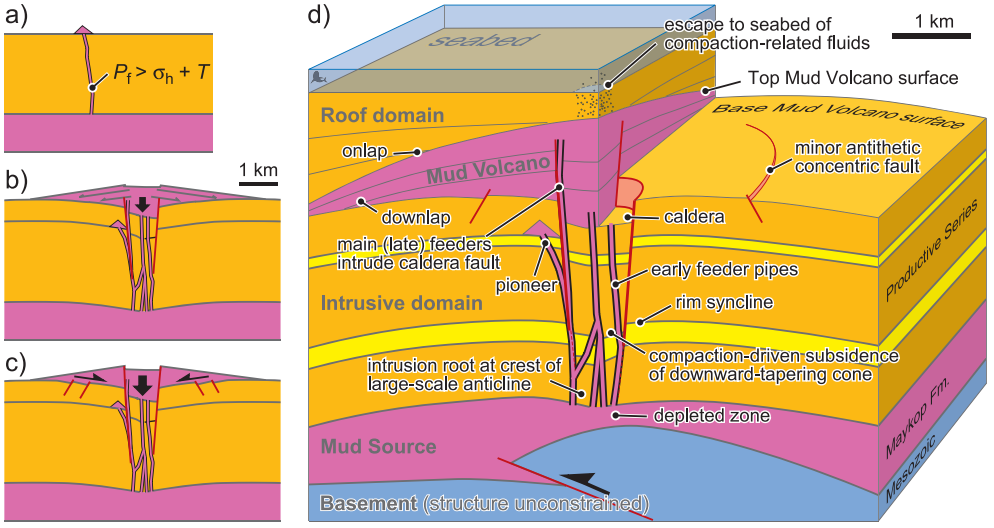

Figure 10. Diagrams of evolution and 3-D structural elements of model for mud volcano systems based on the mapping and interpretation described in this article. (a–c) Evolution through time from initial single pipe, feeding pioneer cone, through collapsed, heavily intruded downward-tapering cone and caldera underlying a sizable biconic edifice. (d) Three-dimensional summary model based on the mud volcano system illustrated in Figures 6–8. P_f = fluid pressure; σ_n = horizontal stress; T = tensile strength of overburden.

(Pickering et al., 1988; Brown, 1990; Graue, 2000; Aminzade et al., 2001; Cartwright and Huuse, 2005). Diatreme or fluidization pipe propagation is initiated and driven by fluid pressure exceeding the tensile strength of the overburden plus minimum horizontal stress (e.g., Jolly and Lonergan, 2002; Seldon and Flemings, 2005). Resulting hydraulic fractures propagate hundreds of meters above the overpressure source and establish a pathway for upward movement of overpressured, fluidized material through the overburden (Morley, 2003). Seismic imaging indicates that they are pipes or laterally restricted fractures in this study area in the order of tens of meters in width. We have not pursued geomechanical aspects of hydrofracturing here. In the Caspian study area, we follow Narimanov (1993) in attributing a significant component of mud fluid pressure to disequilibrium compaction and hydrocarbon generation in the Maykop Formation. Kilometer-scale buckle folding and mud volcanism throughout the South Caspian are broadly contemporaneous (Figure 1) (Yusifov and Rabinowitz, 2004), so a component of tectonic stress may also be important.

Fragments of country rock are common in mud flows at outcrop onshore, indicating that country rock replaced by the mud-filled pipe is transported to the surface by wall rock erosion and entrainment in the mud (Kopf et al., 2003). A component of wall-rock breccia in extruded mud occurs in many mud volcano systems worldwide (e.g., McManus and Tate, 1986; Pickering et al., 1988; Robertson and Kopf, 1998; Kopf, 2002; Clari et al., 2004). Exposed volcanoes and field outcrops onshore show scattered arrays of meter-scale mud edifices (gryphons), demonstrating that there can be several conduits in a small area (Hovland et al., 1997; Planke et al., 2003). Although it must be acknowledged that exposed gryphon swarms are at high structural levels relative to the mud source and, indeed, are sometimes clearly perched on top of kilometer-scale mud volcanoes, we extrapolate the gryphon swarm model to the subsurface. We suggest that numerous pipes repeatedly intrude the overburden at approximately the same location, forming a steep, cylindrical zone of heavily intruded country rock or amalgamated mud pipes. With a high net volume of intruded mud, this cylindrical zone would have low mechanical strength relative to the surrounding in-situ strata. In our model, this steep cylindrical or conic zone of intrusions then undergoes differential compaction, resulting in a downward-tapering conical collapse opening upward into a caldera or sag. Faults and fractures within and on the margins of the cone provide inherent weaknesses that are exploited by later fluidized flows (Kurszlaukis and Barnett, 2003; Morley, 2003). Localization of late fluidized flows on to the faulted margin of a downward-tapering cone and caldera would lead to the late extrusions being centered on the caldera margin, instead of being concentric with the caldera itself. This could account for observed offset between caldera and bicone axes.

In some of the examples mapped here, the Maykop shale isopach map shows a pancakelike depletion zone below the downward-tapering cone. The loss of volume at depth generates a localized basin or rim syncline to a radial distance of 1 km (0.6 mi) or so beyond

the downward-tapering cone margin in the overlying strata (Figure 10b, d).

Concomitant with the growth of the extrusive edifice and the development of the underlying structure, ongoing basin subsidence can bury the edifice, its 3-D geometry reflecting the relative rates of extrusion, sedimentation, and, if relevant, erosion (Jenyon, 1986; Koyi, 1998; Rowan et al., 2003). This gives rise to two scenarios of mud-sourcing reactivation of the deep primary mud source and the remobilization of a buried bicone. We term these two end-member modes of reactivation ''primary'' and ''secondary.'' During primary reactivation, there is renewed flow of mud directly from the source layer at depth, creating a new volcano that is related to the underlying system only in that it shares the same connection to the source. In an application of the passive salt diapir model for irregular margins of aggradational edifices, the pattern of dormancy and reactivation through time, relative to the rate of background sedimentation, will be recorded in a stacking pattern of bicones separated by layers of sediment (Figure 4) or perhaps a single large bicone with interdigitating or corrugated margins. Care should be taken with the description of buried paleovolcanoes as mud chambers (Deville et al., 2003; Yusifov and Rabinowitz, 2004) because it implies subsurface emplacement analogous to pluton intrusion in igneous settings.

In contrast to episodic sediment pulses from the mud-source layer, a second mechanism can be envisaged, although we have not demonstrated its occurrence in this study. If a buried mud volcano has not fully dewatered and compacted, it could be prone to reactivation in a manner similar to shallow salt intrusions (e.g., Rowan et al., 1999). We term such remobilization of a buried constructional edifice ''secondary mud source reactivation.'' Remobilization could be envisaged as a discrete event triggered by some critical degree of burial, seal failure, and flow, or continuous compaction-driven fluid and mud expulsion as during the burial of the underlying volcano. Although the buried edifice, in this case, could indeed be described as a mud chamber sourcing the latter phase of mud volcanism, the chamber is clearly identified as a paleovolcano instead of an intrusion.

IMPLICATIONS FOR RESERVOIR AND DRILLING

Fluid conduits, be they mud volcano feeders or drilled wells, can impact hydrocarbon systems by providing connection between deep fluid sources and shallow reservoirs. The buildup of an impermeable clay cake on the walls of pipes or dikes mimics mud cake buildup in drilled wells and, similarly, could prevent fluid loss into sands within the overburden, sealing shallow reservoirs from the effects of short-term fluctuations in fluid content and pressure in mud feeders (Morley, 2003). However, fresh sand faces will be exposed to the mud feeder system during the propagation of new pipes and faulting associated with the collapse of a downward-tapering cone. Cross-flow between stacked aquifers connected by mud volcano systems in the South Caspian Basin was considered in a basin modeling study by Bredehoeft et al. (1988). They concluded, from a lack of aquifer compartmentalization at a regional scale, that mud volcanoes do not provide permanently open vertical conduits between permeable strata in the Caspian (Bredehoeft et al., 1988). However, over geologic time scales, it is difficult to rule out episodic drawdown of reservoir pressure in the vicinity of mud volcano systems via a temporary connection to shallower aquifers or the surface. Studies elsewhere have shown that increases in mean effective stress can damage porosity and permeability via mechanical compaction (e.g., Chuhan et al., 2002).

Two direct structural impacts on reservoir-quality erosion and replacement of reservoir by intruding mud, and deformation mechanisms are associated with structural collapse. The multiple pipe intrusion model developed in this article suggests that in reservoirs below mud volcanoes, mud-filled pipes or fractures may represent a relatively small proportion of a feeder system volume. In addition to giving rise to the possibility of unintruded reservoir within a mud feeder system, it is also positive in terms of well planning because there would be a chance of drilling through a feeder system without encountering any mud conduit. However, reservoir may be affected by deformation associated by caldera collapse or downfaulting associated with the development of a downward-tapering cone. There may also be a downward flexure associated with mud-source layer deflation (secondary rim syncline) that affects strata some radial distance beyond the margins of the downward-tapering cone. The spatial extent and degree of reservoir degradation depends on the size and amount of curvature imposed on the reservoir by these structures and the mechanical response of the reservoir to this deformation. Effects could range from none (distributed shear with no discernable effect on porosity) to compartmentalization by discrete faults (Troll et al., 2002). The best predictor of a given reservoirs' response to structural collapse will probably

come from geometric calibration against known structural features elsewhere in the same reservoir, for example, comparing structures above a deflation zone against curvatures elsewhere in the reservoir where there are well-controlled dynamic data.

From a drilling perspective, mud volcano systems pose a problem by introducing local uncertainties in pore and fracture pressure. This could become an issue in well design if there were already tight constraints on drillability because of formation pressure, fracture gradient, and length of the open-hole section; a zone of anomalously low fracture strength (e.g., active fluid conduit) could become a zone of uncontrollable losses in the wellbore. Mud volcano systems will not have much impact on vertical wells (exploration or appraisal wells) other than the requirement to drill through paleomud flows that are likely to be compacted and benign. However, mud volcano systems may lie directly in the path of high-inclination production wells that have constrained top-hole location (e.g., a platform) and bottomhole location (target). As mentioned above, if one chose to drill through a downward-tapering cone, one could be fortunate in not encountering a weak mud conduit, but the well would be likely to encounter several faults or fractures associated with the collapse zone (Figure 8), and faults themselves can be a drilling issue if they are critically stressed or have relatively low fracture strength. A feature of the model developed in this study (Figure 10) is that nearly all the subvolcanic structural elements (pipes and collapse-related faults) are contained within the downward-tapering cone. Therefore, this 3-D envelope can be treated in well planning as a no-go zone, or antitarget volume (e.g., Figure 11). This conservative approach has the potential to remove uncertainty associated with mud conduit and fault drillability from well planning at an early phase and could even influence platform location. It does not, however, consider any present-day far-field stress perturbations associated with the presence of the mud volcano system.

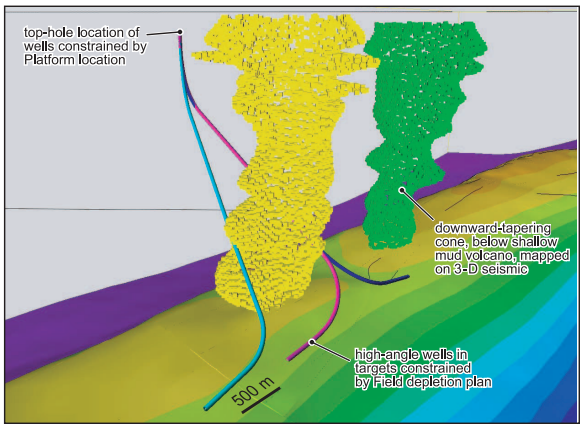

Figure 11. Perspective view of the 3-D structural model based on seismic mapping, looking northeast, used for well planning. Yellow and green data clouds are downward-tapering cones underlying shallow mud volcano edifices. Well planners have used this model to optimize well tracks to avoid intersecting the downward-tapering cones, removing this element of structural and drilling uncertainty. Variation in diameter of the downward-tapering cone with depth reflects variation in seismic data quality and seismic interpreters' uncertainty on the position of the cone.

CONCLUSIONS

We have mapped structural elements ranging from extrusive volcanoes downward through subvolcanic ring complexes to the in-situ mud-source layer. We propose the term ''mud volcano system'' to cover the entire system of allochthonous mud and associated structures, avoiding confusion associated with use of the term ''mud volcano'' when describing subvolcanic structures. An evolutionary model for mud volcano systems in the South Caspian Basin based on this mapping indicates that mud volcano systems of the South Caspian Basin are triggered and driven by hydrofracture instead of reactive exploitation of tectonic structures. This branch of mud volcanism shares little with established salt diapirism models but has geometrical (and probably mechanical) elements in common with igneous systems. We do not suggest that the model developed here applies universally to mud intrusions. It has been demonstrated in different settings that the evolution of mobile mud or shale structures can closely track the geometrical evolution of salt structures (e.g., Morley and Guerin, 1996).

We have illustrated the 3-D structure and described an evolutionary model for mud volcanoes and associated structural elements that connect them to the mud-source layer. Mapped structural elements include early pioneer volcano, downward-tapering cones, calderas, and constructional bicones. Long-lived mud volcano systems can build up a stack of constructional edifices interleaved with nonvolcanic sediment. Buried bicones can be mistaken for the top of salt diapirs or intrusive mud chambers. We recognized these as buried edifices that may occasionally reactivate and perform the function of a secondary mud source.

Some aspects of this work may be relevant to reservoir simulation and well planning. The key elements

of the model in both cases are the description of a downward-tapering cone that contains an assemblage of steep mud intrusions and the structures accommodating the collapse of country rock.

REFERENCES CITED

Allen, M. B., S. J. Vincent, G. I. Alsop, A. Ismail-zadeh, and R. Flecker, 2003, Late Cenozoic deformation in the South Caspian region: Effects of a rigid basement block within a collision zone: Tectonophysics, v. 366, p. 223–239.

Aminzade, F., P. de Groot, T. Berge, and G. Valenti, 2001, Using gas chimneys as an exploration tool: Part 1: World Oil, v. May, p. 50–56.

Bagirov, E., R. Nadirov, and I. Lerche, 1997, Hydrocarbon evolution for a north-south section of the South Caspian Basin: Marine and Petroleum Geology, v. 14, p. 773–854.

Branney, M. J., 1995, Downsag and extension at calderas: New perspectives on collapse geometries from ice-melt, mining and volcanic subsidence: Bulletin of Volcanology, v. 57, p. 303–318.

Bray, C. J., and D. E. Karig, 1985, Porosity of sediments in accretionary prisms and some implications for dewatering processes: Journal of Geophysical Research, v. 90, p. 768–778.

Bredehoeft, J. D., R. D. Djevanshir, and K. R. Belitz, 1988, Lateral fluid flow in a compacting sand-shale sequence: South Caspian Basin: AAPG Bulletin, v. 72, p. 416–424.

Brown, K. M., 1990, The nature and hydrogeological significance of mud diapirs and diatremes for accretionary prisms: Journal of Geophysical Research, v. 95, p. 8969–8982.

Brunet, M. F., M. V. Korotaev, A. V. Ershov, and A. M. Nikishin, 2003, The South Caspian Basin: A review of its evolution from subsidence modelling: Sedimentary Geology, v. 156, p. 119–148.

Cartwright, J., and M. Huuse, 2005, 3D seismic technology: The geological ''Hubble:'' Basin Research, v. 17, p. 1–20.

Chuhan, F. A., A. Kjeldstad, K. Bjørlykke, and K. Høeg, 2002, Porosity loss in sand by grain crushing— Experimental evidence and relevance to reservoir quality: Marine and Petroleum Geology, v. 19, p. 39–53.

Clari, P., S. Cavagna, L. Martire, and J. Hunziker, 2004, A Miocene mud volcano and its plumbing system: A chaotic complex revisited (Monferrato, NW Italy): Journal of Sedimentary Research, v. 74, p. 662–676.

Cole, J. W., D. M. Milner, and K. D. Spinks, 2005, Calderas and caldera structures: A review: Earth Science Reviews, v. 69, p. 1–26.

Cooper, C., 2001a, Mud volcanoes of Azerbaijan visualized using 3D seismic depth cubes: The importance of overpressured fluid and gas instead of non-existent diapirs (abs.): Proceedings of the European Association of Geoscientists and Engineers Conference on Subsurface Sediment Mobilisation, Gent, Belgium, September 2001, p. 71.

Cooper, C., 2001b, Mud volcanoes of the South Caspian Basin— Seismic data and implications for hydrocarbon systems (extended abstract): AAPG Convention Abstracts, CD-ROM, 5 p.

Davies, R. J., and S. A. Stewart, 2005, Emplacement of giant mud volcanoes in the South Caspian Basin: 3D seismic reflection imaging of their root zones: Journal of the Geological Society (London), v. 162, p. 1–4.

Davies, R. J., S. A. Stewart, J. A. Cartwright, M. Lappin, R. Johnston, and S. Fraser, 2004, 3D seismic technology: Are we realising its full potential?, *in* R. J. Davies, J. A. Cartwright, S. A. Stewart, M. Lappin, and J. R. Underhill, eds., 3D seismic technology: Application to the exploration of sedimentary basins: Geological Society (London) Memoir 29, p. 1–9.

Deville, E., A. Battani, R. Griboulard, S. Guerlais, J. P. Herbin, J. P. Houzay, C. Muller, and A. Prinzhoffer, 2003, The origin and processes of mud volcanism: New insights from Trinidad, *in* P. Van Rensbergen, R. R. Hillis, A. J. Maltman, and C. K. Morley, eds., Subsurface sediment mobilization: Geological Society (London) Special Publication 216, p. 475–490.

Dionne, J.-C., 1973, Monroes: A type of so-called mud volcanoes in tidal flats: Journal of Sedimentary Petrology, v. 43, p. 848–856.

Ebrom, D., P. Heppard, L. Thomsen, M. Mueller, T. Harrold, L. Phillip, and P. Watson, 2004, Effective stress and minimum velocity trends (abs.): Society of Exploration Geophysicists Technical Program Expanded Abstracts, p. 1615–1618.

Etiope, G., A. Feyzullayev, C. L. Baciu, and A. V. Milkov, 2004, Methane emission from mud volcanoes in eastern Azerbaijan: Geology, v. 32, p. 465–468.

Fowler, S. R., J. Mildenhall, S. Zalova, G. Riley, G. Elsley, A. Desplanques, and F. Guliyev, 2000, Mud volcanoes and structural development on Shah Deniz: Journal of Petroleum Science and Engineering, v. 28, p. 189–206.

Francis, E. H., 1970, Bedding in Scottish (Fifeshire) tuff-pipes and its relevance to maars and calderas: Bulletin of Volcanology, v. 34, p. 697–712.

Freeman, P. S., 1968, Exposed middle Tertiary mud diapirs and related features in south Texas, *in* J. Braunstein and G. D. O'Brien, eds., Diapirism and diapirs: AAPG Memoir 8, p. 162–182.

Ge, H., and M. P. A. Jackson, 1998, Physical modelling of structures formed by salt withdrawal: Implications for deformation caused by salt dissolution: AAPG Bulletin, v. 81, p. 228–250.

Graue, K., 2000, Mud volcanoes in deepwater Nigeria: Marine and Petroleum Geology, v. 17, p. 959–974.

Hovland, M., A. Hill, and D. Stokes, 1997, The structure and geomorphology of the Dashgil mud volcano, Azerbaijan: Geomorphology, v. 21, p. 1–15.

Inan, S., M. N. Yalcin, I. S. Guliev, K. Kuliev, and A. A. Feizullayev, 1997, Deep petroleum occurrences in the lower Kura depression, south Caspian Basin, Azerbaijan: An organic geochemical and basin modelling study: Marine and Petroleum Geology, v. 14, p. 731–762.

Jackson, J., K. Priestley, M. Allen, and M. Berberian, 2002, Active tectonics of the South Caspian Basin: Geophysical Journal International, v. 148, p. 214–245.

Jakubov, A. A., A. A. Ali-Zade, and M. M. Zeinalov, 1971, Mud volcanoes of the Azerbaijan SSR: Baku, Publication House Academy of Science, Azerbaijan SSR, 257 p.

Jenyon, M. K., 1986, Salt tectonics: London, Elsevier, 198 p.

Johnson, S. E., K. L. Schmidt, and M. C. Tate, 2002, Ring complexes in the Peninsular Ranges batholith, Mexico and the U.S.A.: Magma plumbing systems in the middle and upper crust: Lithos, v. 61, p. 187–208.

Jolly, R. J. H., and L. Lonergan, 2002, Mechanisms and controls on the formation of sand intrusions: Journal of the Geological Society (London), v. 159, p. 605–617.

Judd, A. G., 2005, Gas emissions from mud volcanoes: Significance to global climate change, *in* G. Martinelli and B. Panahi, eds., Mud volcanoes, geodynamics and seismicity: Proceedings of the North Atlantic Treaty Organization (NATO) Advanced Research Workshop on Mud Volcanism, Geodynamics and Seismicity, Baku, Azerbaijan, May 2003: NATO Science Series: IV: Earth and Environmental Sciences, v. 51.

Knapp, C. C., J. H. Knapp, and J. A. Connor, 2004, Crustal-scale structure of the South Caspian Basin revealed by deep seismic reflection profiling: Marine and Petroleum Geology, v. 21, p. 1073–1081.

Kopf, A. J., 2002, Significance of mud volcanism: Reviews of Geophysics, v. 40, p. 1–52.
Kopf, A. J., and J. H. Behrmann, 2000, Extrusion dynamics of mud volcanoes on the Mediterranean Ridge accretionary complex, *in* B. C. Vendeville, Y. Mart, and J. L. Vigneresse, eds., Salt, shale and igneous diapirs in and around Europe: Geological Society (London) Special Publication 174, p. 169–204.
Kopf, A., D. Klaeschen, and J. Mascle, 2001, Extreme efficiency of mud volcanism in dewatering accretionary prisms: Earth and Planetary Science Letters, v. 189, p. 295–313.
Kopf, A., A. Deyhle, V. Y. Lavrushin, B. G. Polyak, J. M. Gieskes, G. I. Buachidze, K. Wallmann, and A. Eisenhauer, 2003, Isotopic evidence (He, B, C) for deep fluid and mud mobilization from mud volcanoes in the Caucasus continental collision zone: International Journal of Earth Sciences, v. 92, p. 407–425.
Koyi, H., 1998, The shaping of salt diapirs: Journal of Structural Geology, v. 20, p. 321–338.
Kurszlaukis, S., and W. P. Barnett, 2003, Volcanological and structural aspects of the Venetia kimberlite cluster— A case study of South African kimberlite maar-diatreme volcanoes: South African Journal of Geology, v. 106, p. 165–192.
Kvenvolden, K. A., and B. W. Rogers, 2005, Gaia's breath— Global methane exhalations: Marine and Petroleum Geology, v. 22, p. 579–590.
Lance, S., P. Henry, X. Le Pichon, S. Lallemant, H. Chamley, F. Rostek, J. C. Faugeres, E. Gonthier, and K. Olu, 1998, Submersible study of mud volcanoes seaward of the Barbados accretionary wedge: Sedimentology, structure and rheology: Marine Geology, v. 145, p. 255–292.
Lipman, P. W., 2000, Calderas, *in* H. Sigurdsson, ed., Encyclopedia of volcanoes: San Francisco, Academic Press, p. 643–662.
Lorenz, V., 1975, Formation of phreatomagmatic maar-diatreme volcanoes and its relevance to Kimberlite diatremes: Physics and Chemistry of the Earth, v. 9, p. 17–27.
Maione, S. J., 2001, Discovery of ring faults associated with salt withdrawal basins, Early Cretaceous age, in the east Texas basin: The Leading Edge, v. 20, p. 818–829.
Malthe-Sørenssen, A., T. Walmann, B. Jamtveit, J. Feder, and T. Jøssang, 1999, Simulation and characterization of fracture patterns in glaciers: Journal of Geophysical Research— Solid Earth, v. 104, p. 23,157–23,174.
McManus, J., and R. B. Tate, 1986, Mud volcanoes and the origin of certain chaotic deposits in Sabah, east Malaysia: Geological Society of Malaysia Bulletin, v. 19, p. 193–205.
Milkov, A. V., 2000, Worldwide distribution of submarine mud volcanoes and associated gas hydrates: Marine Geology, v. 167, p. 29–42.
Morley, C. K., 2003, Outcrop examples of mudstone intrusions from the Jerudong anticline, Brunei Darussalam and inferences for hydrocarbon reservoirs, *in* P. Van Rensbergen, R. R. Hillis, A. J. Maltman, and C. K. Morley, eds., Subsurface sediment mobilization: Geological Society (London) Special Publication 216, p. 381–394.
Morley, C. K., and G. Guerin, 1996, Comparison of gravity-driven deformation styles and behaviour associated with mobile shales and salt: Tectonics, v. 15, p. 1154–1170.
Murton, B. J., and J. Biggs, 2003, Numerical modelling of mud volcanoes and their flows using constraints from the Gulf of Cadiz: Marine Geology, v. 195, p. 223–236.
Narimanov, A. A., 1993, The petroleum systems of the South Caspian Basin, *in* A. G. Dore, J. H. Augustson, C. Hermanrud, D. J. Stewart, and O. Sylta, eds., Basin modeling advances and applications: Norwegian Petroleum Forening Special Publication 3, 599–608.
Pickering, K. T., S. M. Agar, and Y. Ogawa, 1988, Genesis and deformation of mud injections containing chaotic basalt-limestone-chert associations: Examples from the southwest Japan forearc: Geology, v. 16, p. 881–885.
Planke, S., H. Svensen, M. Hovland, D. A. Banks, and B. Jamtveit, 2003, Mud and fluid migration in active mud volcanoes in Azerbaijan: Geo-Marine Letters, v. 23, p. 258–268.
Robertson, A. H. F., and A. J. Kopf, 1998, Tectonic setting and processes of mud volcanism on the Mediterranean Ridge accretionary complex: Evidence from Leg 160, *in* A. H. F. Robertson, K.-C. Emeis, C. Richter, and A. Camerlenghi, eds., Proceedings of the Ocean Drilling Program, Scientific Results, v. 160, p. 665–680.
Roche, O., T. H. Druitt, and O. Merle, 2000, Experimental study of caldera formation: Journal of Geophysical Research— Solid Earth, v. 105B, p. 395–416.
Rowan, M. G., M. P. A. Jackson, and B. D. Trudgill, 1999, Salt-related fault families and fault welds in the northern Gulf of Mexico: AAPG Bulletin, v. 83, p. 1454–1484.
Rowan, M. G., T. F. Lawton, K. A. Giles, and R. A. Ratliff, 2003, Near-salt deformation in La Popa basin, Mexico, and the northern Gulf of Mexico: A general model for passive diapirism: AAPG Bulletin, v. 87, p. 733–756.
Seldon, B., and P. B. Flemings, 2005, Reservoir pressure and seafloor venting: Predicting trap integrity in a Gulf of Mexico turbidite minibasin: AAPG Bulletin, v. 89, p. 193–209.
Stewart, S. A., and J. A. Argent, 2000, Relationship between polarity of extensional fault arrays and the presence of detachments: Journal of Structural Geology, v. 22, p. 693–711.
Talbot, C. J., and V. von Brunn, 1989, Melanges, intrusive and extrusive sediments and hydraulic arcs: Geology, v. 17, p. 446–448.
Troll, V. R., T. R. Walter, and H. U. Schmincke, 2002, Cyclic caldera collapse: Piston or piecemeal subsidence? Field and experimental evidence: Geology, v. 30, p. 135–138.
Trusheim, F., 1960, Mechanism of salt migration in northern Germany: AAPG Bulletin, v. 44, p. 1519–1540.
Van Rensbergen, P., C. K. Morley, D. W. Ang, T. Q. Hoan, and N. T. Lam, 1999, Structural evolution of shale diapirs from reactive rise to mud volcanism: 3D seismic data from the Baram delta, offshore Brunei Darussalam: Journal of the Geological Society (London), v. 156, p. 633–650.
Vendeville, B. C., 2002, A new interpretation of Trusheim's classic model of salt-diapir growth: Transactions, Gulf Coast Association of Geological Societies, v. 52, p. 943–952.
Walker, G. P. L., 1988, Three Hawaiian calderas: An origin through loading by shallow intrusions?: Journal of Geophysical Research— Solid Earth, v. 93B, p. 14,773–14,784.
Yeilding, C. A., and C. J. Travis, 1997, Nature and significance of irregular geometries at the salt-sediment interface: Examples from the deepwater Gulf of Mexico (abs.): AAPG Annual Meeting Program, v. 6, p. A128.
Yusifov, M., and P. D. Rabinowitz, 2004, Classification of mud volcanoes in the South Caspian Basin, offshore Azerbaijan: Marine and Petroleum Geology, v. 21, p. 965–975.